

Supplementary Material

Sources and oxidative potential of water-soluble humic-like substances (HULIS_{WS}) in fine particulate matter (PM_{2.5}) in Beijing

Yiqiu Ma^{1,2}, Yubo Cheng², Xinghua Qiu^{*,1}, Gang Cao³, Yanhua Fang¹, Junxia Wang¹, Tong Zhu¹, Jianzhen Yu⁴, Di Hu^{*,2,5,6}

¹State Key Joint Laboratory for Environmental Simulation and Pollution Control, College of Environmental Sciences and Engineering, Peking University, Beijing 100871, P. R. China

²Department of Chemistry, Hong Kong Baptist University, Kowloon Tong, Kowloon, Hong Kong, P. R. China

³Harbin Institute of Technology (Shenzhen), Shenzhen Key Laboratory of Organic Pollution Prevention and Control, Shenzhen 518055, P. R. China

⁴Department of Chemistry, Hong Kong University of Science and Technology, Clear Water Bay, Kowloon, Hong Kong, P. R. China

⁵State Key Laboratory of Environmental and Biological Analysis, Hong Kong Baptist University, Kowloon Tong, Kowloon, Hong Kong, P. R. China

⁶HKBU Institute of Research and Continuing Education, Shenzhen Virtual University Park, Shenzhen, 518057, P. R. China

Correspondence to: Xinghua Qiu (xhqi@pku.edu.cn); Di Hu (dihu@hkbu.edu.hk)

Content of this file

Section S1. HPLC-ELSD analysis of total HULIS_{WS}

Section S2. GC-MS analysis of individual HULIS_{WS} species

Section S3. Positive Matrix Factorization (PMF) analysis

Section S4. Calculation of particle-phase liquid water content (LWC_p) and particle acidity (H_p⁺)

Table S1. Concentrations of individual HULIS_{WS} species during the heating and non-heating seasons

Table S2. Multilinear regression analysis of PMF-resolved HULIS_{WS} from vehicle emissions (HULIS_{WS_VE}), particle acidity (H_p⁺), particle-phase liquid water content (LWC_p), and particle-phase SO₄²⁻, NO_x and O₃

Table S3. Multilinear regression analysis of PMF-resolved HULIS_{WS} from secondary aerosol formation (HULIS_{WS_SEC}), particle acidity (H_p⁺), particle-phase liquid water content (LWC_p), and particle-phase SO₄²⁻, NO_x and O₃

Figure S1. The comparison of GC-MS peak intensity of HULIS_{WS} species eluted by methanol and basic methanol

Figure S2. Difference of individual HULIS_{WS} species between the heating and non-heating seasons

Figure S3. Relative source intensities of PMF source profiles

Figure S4. PMF-predicted versus measured concentrations of total HULIS_{WS} and HULIS_{WS}-associated DTT activity

Figure S5. Total HULIS_{WS} versus hopanes and levoglucosan

Figure S5. Temporal variation of gas-phase NO_x concentration in Beijing during 2012-2013

Figure S6. Temporal variation for gas-phase O₃ concentration in Beijing during 2012-2013

Section S1. HPLC-ELSD analysis of total HULIS_{WS}.

Total HULIS_{WS} was analyzed by a high-performance liquid chromatography system (HPLC, ThermoFisher Scientific, Waltham, MA, USA) coupled with an evaporative light scattering detector (Alltech ELSD 3300, Grace, Houston, TX, USA). Detailed method was provided in Lin et al. (2010) Since there is no requirement for further separation, a polyaryletheretherketone tube (15 m, 0.127 mm i.d., Alltech, Dearfield, IL, USA) instead of analytical column was used to connect the HPLC injector port and ELSD). HULIS_{WS} was eluted by isocratic elution with acetonitrile: distilled deionized water (1:4, vol/vol) at a rate of 0.6 mL min⁻¹. The ELSD was operated at a N₂ flow rate of 1.5 L min⁻¹ and a drift tubing temperature of 90°C. The recoveries of representative HULIS_{WS} species were provided in Lin et al. (2010)

42 **Section S2. GC-MS analysis of individual HULIS_{WS} species.**

43 Individual HULIS_{WS} species were analyzed using gas chromatography-mass spectrometry (GC-MS; Agilent 7890A-5975C,
44 Santa Clara, CA, USA) in electron ionization (EI) mode. A HP-5MS column (30 m, 250 μm i.d., 0.25 μm film thickness,
45 Agilent, Santa Clara, CA, USA) was used to separate individual species. Two microliter of sample was injected into GC
46 injection in splitless mode. The GC oven temperature program was set as follows: held at 80°C for 5 min; 3°C min⁻¹ to 200°C
47 and held for 2 min; 15°C min⁻¹ to 300°C and held for 15 min. For most compounds with authentic standards, they were
48 identified and quantified by comparison to the standards. For terephthalic acid, 2-hydroxybenzoic acid, and 1,2,3-/1,2,4-
49 benzenetricarboxylic acids, which were lack of authentic standards, isophthalic acid, 3-hydroxybenzoic acid, and 1,3,5-
50 benzenetricarboxylic acid were used as surrogate for the calibration and recovery, respectively. Similarly, for SOA markers,
51 surrogate compounds with similar functional groups were used for calibration and they were determined following the
52 procedure described in Hu et al. (2008). Recoveries for all measured species were within 72%-106%.

53 **Section S3. Positive Matrix Factorization (PMF) analysis.**

54 PMF is a widely used receptor model for the source apportionment of fine particulate matter (PM_{2.5}). In this model, the original
55 data matrix X could be divided into a factor contribution matrix G and a factor profile matrix F :

56
$$X = G \times F + \varepsilon$$

$$\begin{matrix} m \times n & m \times p & p \times n & m \times n \end{matrix}$$

57 where n stands for the sample number, m stands for the species number, p refers to the number of factors in PMF solution, ε
58 refers to a residual matrix.

59 During calculation, the sum of scaled residual Q was minimized:

60
$$Q = \sum_{i=1}^m \sum_{j=1}^n \left(\frac{e_{ij}}{\sigma_{ij}} \right)^2$$

61 where e_{ij} is the residual of each sample, and σ_{ij} is the uncertainty in the j^{th} species for the sample i .

62 In this study, a total of 66 samples and 13 species was included in the final PMF solution. The uncertainty setting was
63 referred to Hu et al.³ Briefly, the uncertainties of total HULIS_{WS}, DTT activity, major ions (Mg²⁺, Ca²⁺, NH₄⁺, SO₄²⁻, and nss-
64 Cl⁻), SOA marker (MonoT) and individual HULIS_{WS} species (4M5NC, 3M6NC, 123Ben, 124Ben, and TPha) were set as 0.4
65 of average annual value. Hopane and Levoglucosan (LevoG) were set as 0.2 of average annual value. The optimal PMF
66 solution had five factors with 20% of extra modeling uncertainty.

67 **Section S3. Calculation of particle-phase liquid water content (LWC_p) and particle acidity (H_p⁺).**

68 LWC_p was associated to both organic (LWC_{org}) and inorganic components (LWC_{inorg}) in PM_{2.5}. The LWC_{org} was calculated
69 using the following equation:

70
$$LWC_{org} = \frac{m_{org} \rho_w}{\rho_{org}} \frac{k_{org}}{(1/RH - 1)}$$

71 where m_{org} is the concentration of organic matter (OM), and in this paper, 1.98 and 1.50 were adopted for OM/OC ratio in the
72 heating and non-heating seasons, respectively.⁴ ρ_w and ρ_{org} are the densities of water and organic, with values of 1 g cm⁻³ and
73 1.4 g cm⁻³, respectively.⁵ k_{org} is the organic hygroscopicity parameter ($k_{org}=0.1$),⁶ and RH is the relative humidity (%).

74 Particle acidity (H_p^+) was calculated using the following equation:

75
$$H_p^+ = \frac{1000H_{air}^+}{LWC_{org} + LWC_{inorg}}$$

76 where H_p^+ (mol/L) is the concentration of hydronium ion in the aqueous solution, interpreted as particle acidity. H_{air}^+ and
77 LWC_{inorg} were calculated by ISORROPIA-II using inorganic ions (Na^+ , SO_4^{2-} , NH_4^+ , Cl^- , Ca^{2+} , K^+ , and Mg^{2+}), RH and
78 temperature as the input

Table S1. Concentrations of individual HULIS_{WS} species during the heating and non-heating seasons

Concentration (ng m ⁻³)	Heating season			Non-heating season		
	Mean	Median	Range	Mean	Median	Range
<i>Individual HULIS_{WS} species</i>						
adipic acid	6.59	3.50	0.91 – 25.5	5.28	4.40	2.01 – 17.7
pimelic acid	2.94	1.77	0.41 – 9.57	2.50	2.21	0.86 – 11.5
vanillic acid	5.88	6.32	0.47 – 12.9	1.28	0.60	n.d. – 10.6
azelaic acid	13.7	10.3	1.14 – 35.5	14.9	13.9	3.86 – 55.2
syringic acid	7.04	4.59	0.38 – 16.5	2.08	1.04	0.29 – 16.0
2-hydroxybenoic acid	6.70	5.40	0.71 – 22.4	1.00	0.69	n.d. – 3.26
3-hydroxybenoic acid	6.03	4.96	0.54 – 21.1	1.03	0.76	n.d. – 6.97
4-hydroxybenoic acid	19.3	13.7	0.99 – 57.6	4.39	1.74	0.47 – 63.3
phthalic acid	54.4	25.0	6.55 – 424	22.0	23.8	6.88 – 69.4
isophthalic acid	4.77	3.29	0.64 – 17.8	2.87	2.30	1.06 – 14.9
terephthalic acid	150	97.7	17.0 – 411	98.1	79.6	7.30 – 372
4-nitrophenol	35.1	27.7	1.49 – 105	2.86	1.56	0.45 – 14.5

4-nitrocatechol	27.1	20.6	0.62 – 103	2.91	1.54	0.50 – 28.1
2-hydroxy-5-nitrobenzoic acid	8.50	8.60	0.33 – 23.8	6.38	8.12	0.72 – 15.8
2-methyl-4-nitrophenol	27.2	24.8	1.47 – 56.9	1.91	0.85	0.32 – 9.68
4-methyl-5-nitrocatechol	7.38	7.94	0.26 – 17.6	0.51	n.d.	n.d. – 8.70
3-methyl-6-nitrocatechol	18.6	16.6	0.51 – 54.5	2.25	1.47	n.d. – 13.7
1,2,3-benzenetricarboxylic acid	27.3	12.6	2.24 – 168	16.2	13.2	n.d. – 65.2
1,2,4-benzenetricarboxylic acid	22.7	11.9	1.98 – 114	13.7	11.5	4.09 – 43.3
1,3,5-benzenetricarboxylic acid	5.95	0.98	0.23 – 134	1.35	0.93	0.26 – 4.94
Σ HULIS _{WS-quantified}	458	368	39.62– 1657	203	178	41.9 – 782
<i>SOA tracers</i>						
3-hydroxyglutaric acid	3.66	3.50	0.36 – 9.77	1.81	1.84	0.71 – 4.85
3-acetylpentanedioic acid	2.47	1.71	n.d. – 8.40	4.44	3.83	1.16 – 10.33
3-hydroxy-4,4-dimethylglutaric acid	1.06	0.80	n.d. – 3.01	1.16	1.04	0.37 – 3.11
3-Isopropylpentanedioic acid	4.01	3.34	n.d. – 14.09	5.34	5.11	1.02 – 11.80
3-methyl-1,2,3-butanetricarboxylic acid	1.26	1.05	n.d. – 3.30	4.09	3.15	1.09 – 9.80

n.d. : not detected.

Table S2. Multilinear regression analysis of PMF-resolved HULIS_{WS} from vehicle emissions (HULIS_{WS_VE}), particle acidity (H_p⁺), particle-phase liquid water content (LWC_p), and particle-phase SO₄²⁻, NO_x and O₃

Variable	β-coefficient	Standard error	t value	p value
Intercept	0.337	0.220	1.530	0.131
H _p ⁺	-0.113	0.508	-0.223	0.824
LWC _p	-0.008	0.008	-0.972	0.335
SO ₄ ²⁻	0.018	0.013	1.381	0.172
NO _x	0.012	0.003	4.254	0.000
O ₃	-0.013	0.004	-3.008	0.004

Table S3. Multilinear regression analysis of PMF-resolved HULIS_{WS} from secondary aerosol formation (HULIS_{WS_SEC}), particle acidity (H_p⁺), particle-phase liquid water content (LWC_p), and particle-phase SO₄²⁻, NO_x and O₃

Variable	β-coefficient	Standard error	t value	p value
Intercept	-0.031	0.357	-0.088	0.930
H _p ⁺	1.291	0.822	1.571	0.121
LWC _p	0.026	0.013	1.997	0.050
SO ₄ ²⁻	0.066	0.021	3.227	0.002
NO _x	-0.001	0.005	-0.267	0.790
O ₃	0.028	0.007	3.942	0.000

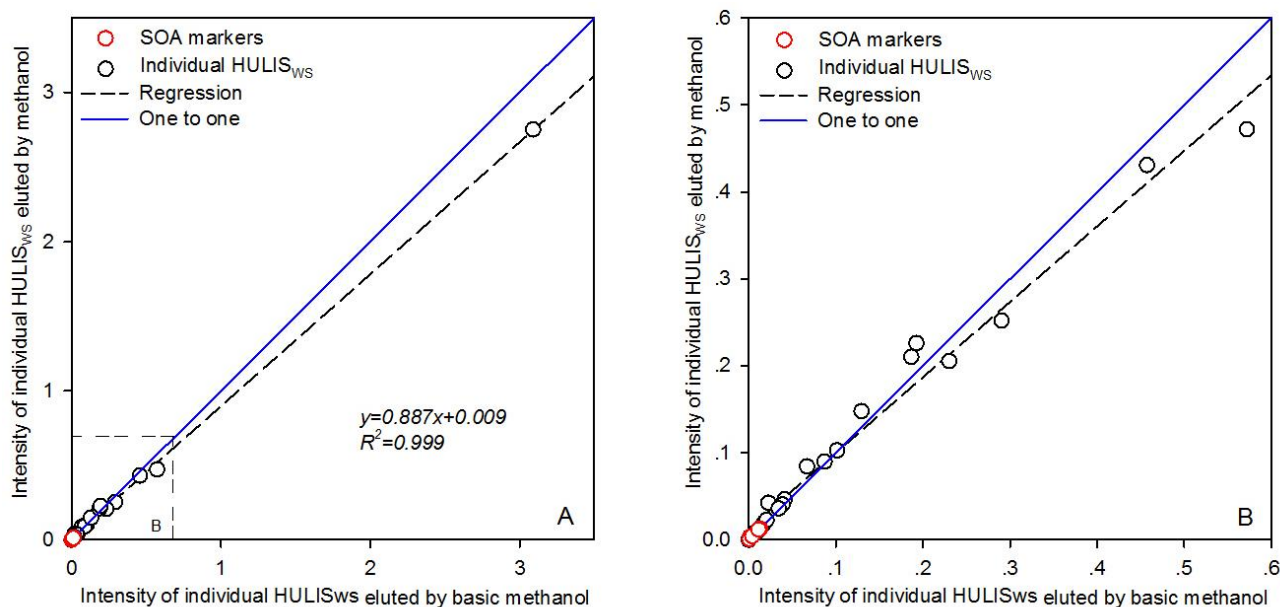


Figure S1. The comparison of GC-MS peak intensity of HULIS_{WS} species eluted by methanol and basic methanol (panel B is the magnification of panel A with the intensity below 0.6)

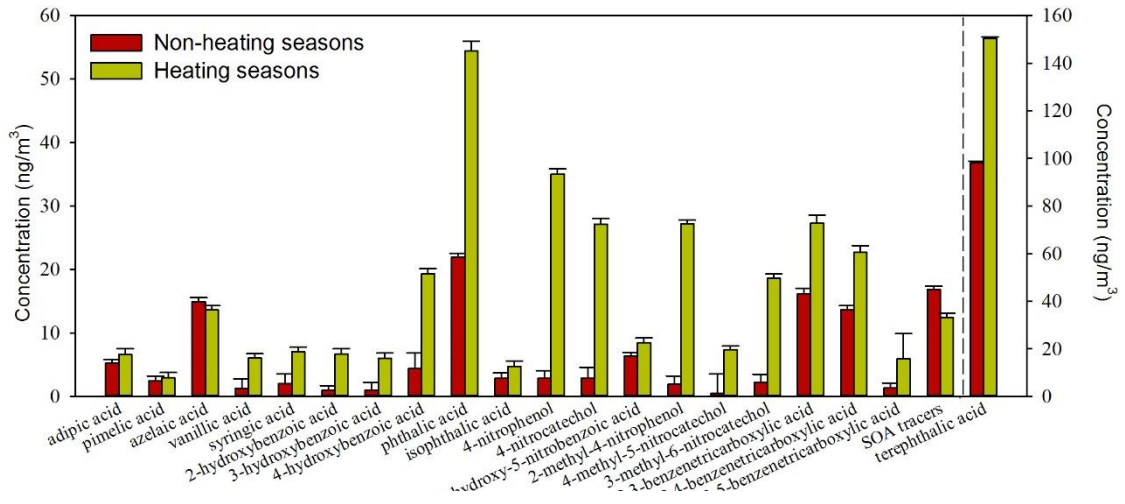


Figure S2. Difference of individual HULIS_{ws} species between the heating and non-heating seasons.

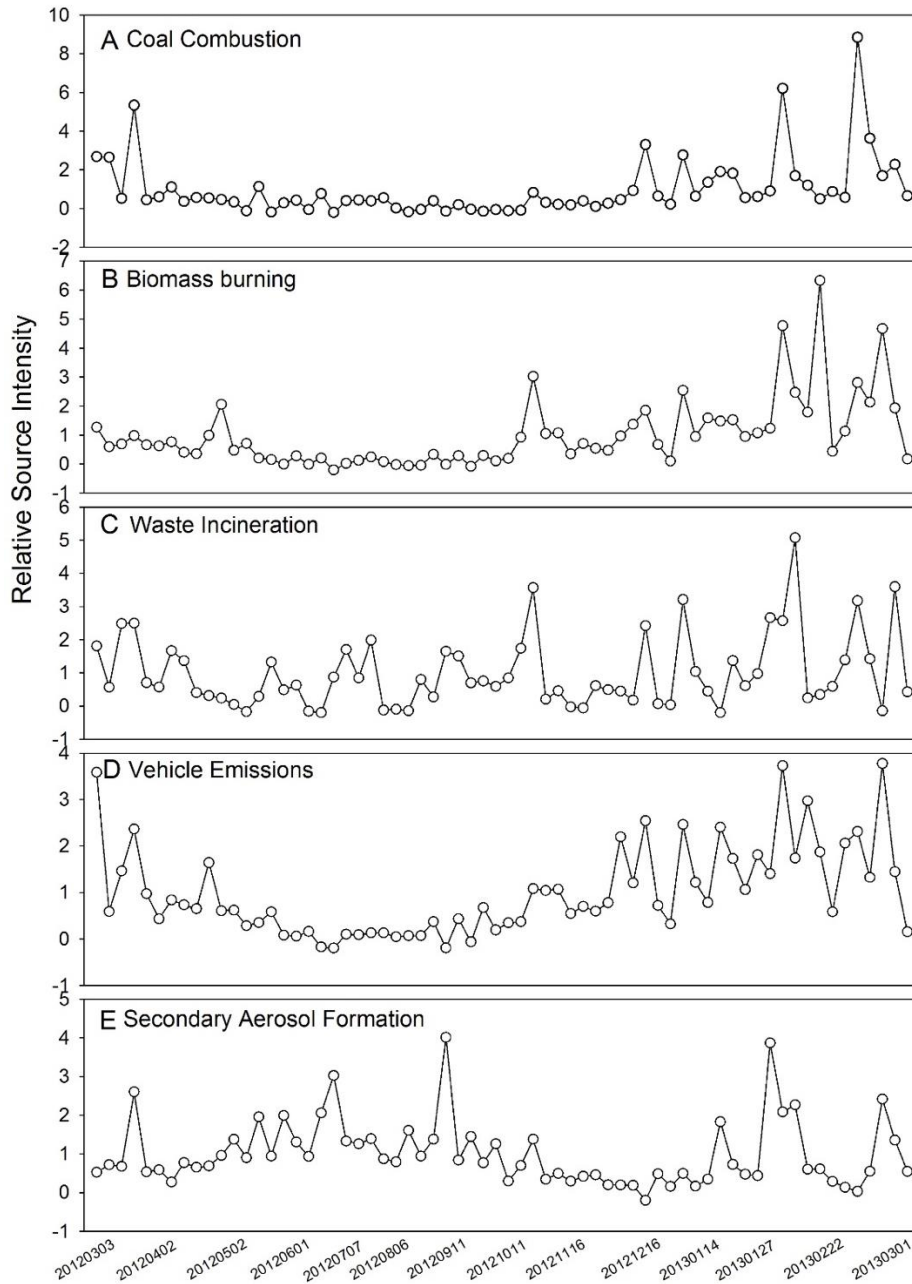


Figure S3. Relative source intensities of PMF source profiles.

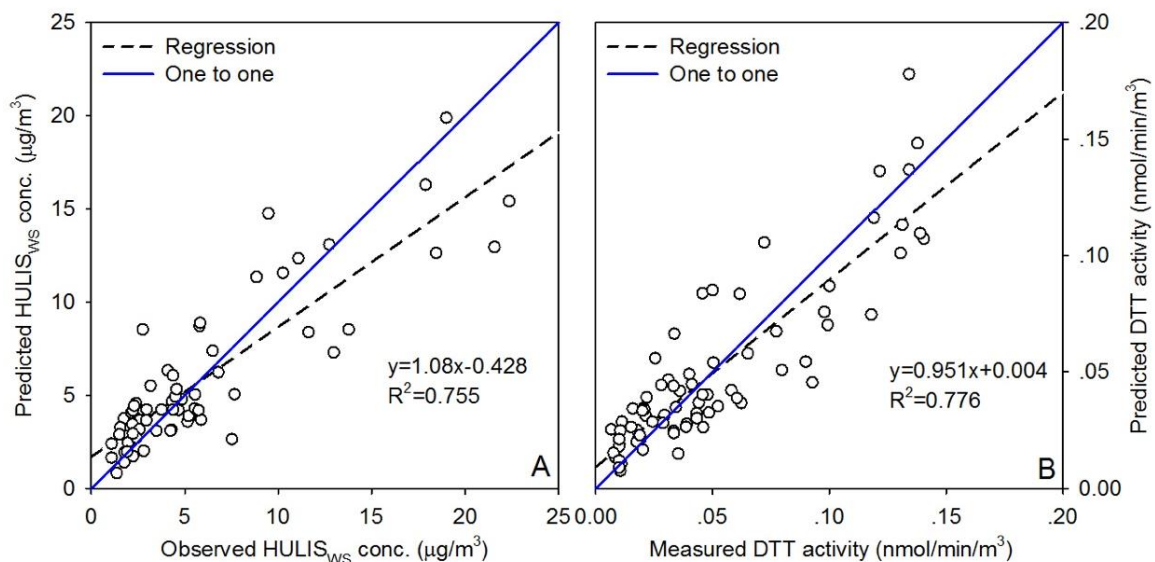


Figure S4. PMF-predicted versus measured concentrations of total HULIS_{WS} (panel A) and HULIS_{WS}-associated DTT activity (panel B).

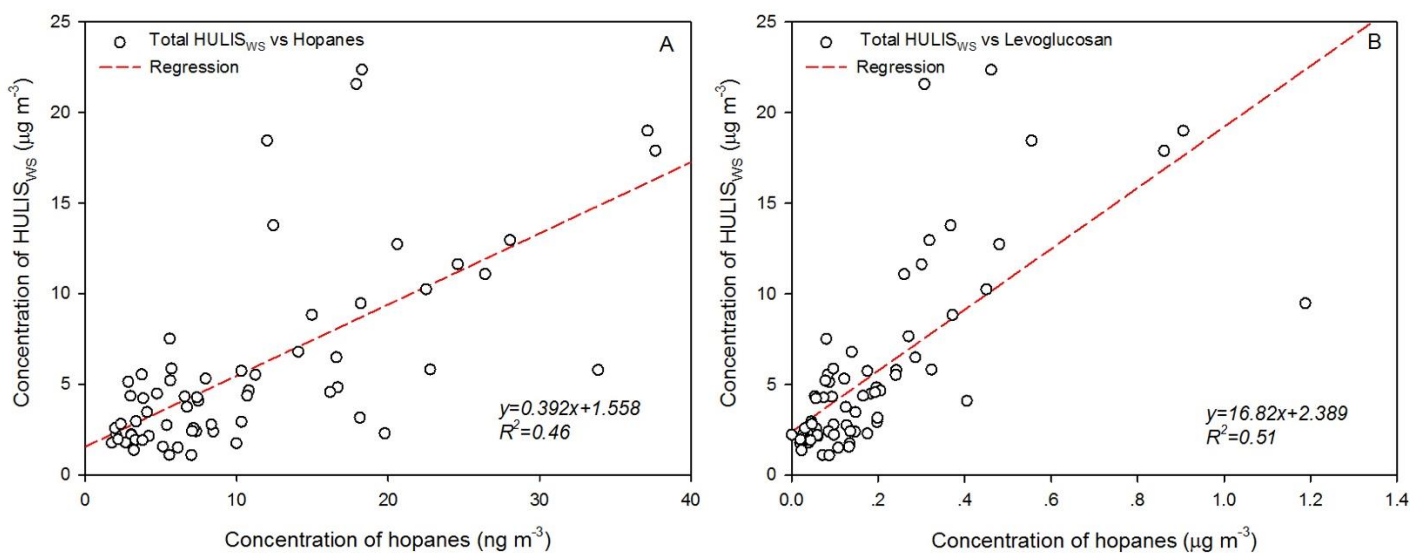


Figure S5. Total HULIS_{WS} versus hopanes (panel A) and levoglucosan (panel B)

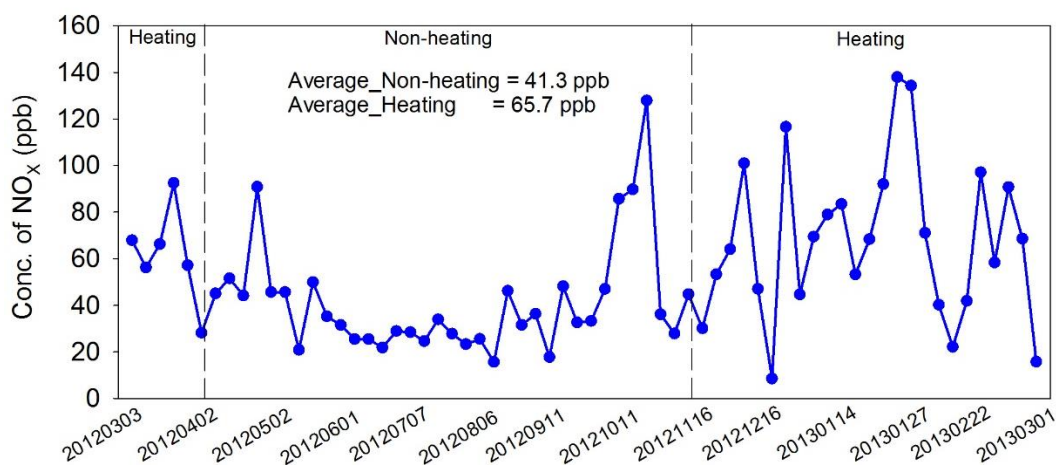


Figure S6. Temporal variation for gas-phase NO_x concentration in Beijing during 2012-2013.

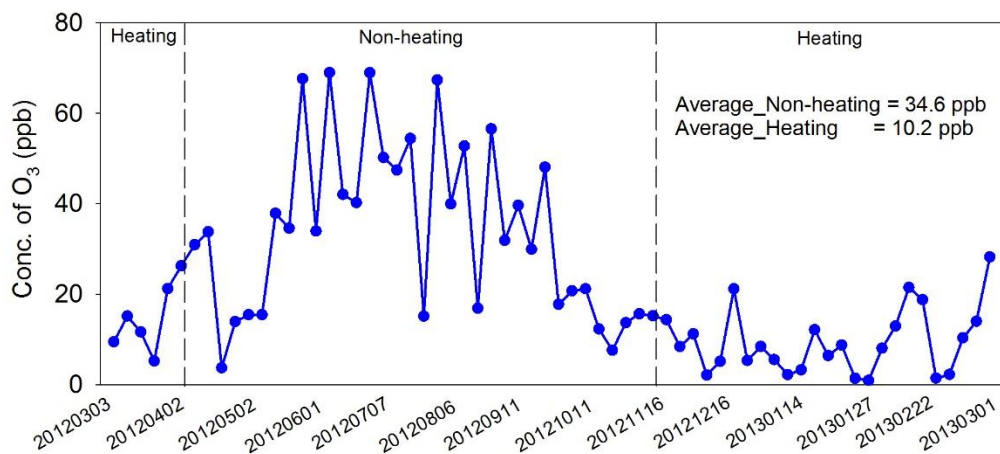


Figure S7. Temporal variation for gas-phase O₃ concentration in Beijing during 2012-2013.

References:

Hu, D., Bian, Q., Li, T. W. Y., Lau, A. K. H. and Yu, J. Z.: Contributions of isoprene, monoterpenes, β -caryophyllene, and toluene to secondary organic aerosols in Hong Kong during the summer of 2006, *J. Geophys. Res. Atmos.*, 113(22), D22206, 2008.

Lin, P., Huang, X. F., He, L. Y. and Zhen Yu, J.: Abundance and size distribution of HULIS in ambient aerosols at a rural site in South China, *J. Aerosol Sci.*, 41(1), 74–87, 2010.